Journal of Materials Chemistry C

Accepted Manuscript

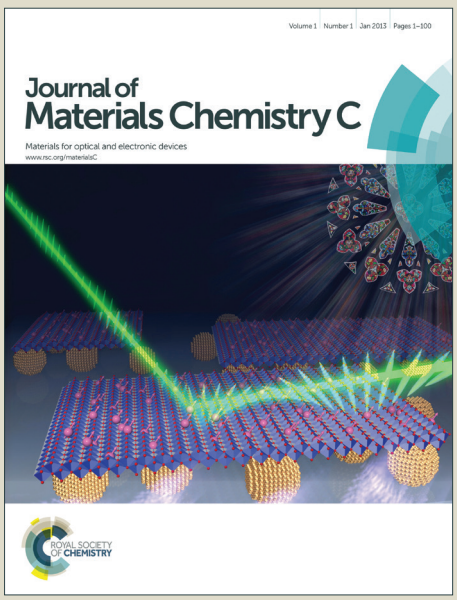

ROYAL SOCIETY OF CHEMISTRY

www.rsc.org/materialsC

Cite this: DOI: 10.1039/c0xx00000x

www.rsc.org/xxxxxx

Paper

Synthesis and properties of azothiazole based π-conjugated polymers

Zhuangqing Yan,[a] Bin Sun,[a] Chang Guo[a] and Yuning Li*[a]

Received (in XXX, XXX) Xth XXXXXXXXX 20XX, Accepted Xth XXXXXXXXX 20XX
DOI: 10.1039/b000000x

In this study, azothiazole, namely (*E*)-1,2-di(thiazol-2-yl)diazene), is used as a building block to construct π-conjugated polymer semiconductors. It is found that azothiazole is a strong electron withdrawing moiety and suitable as an electron acceptor unit to form donor-acceptor (D-A) polymers. Two D-A polymers comprising azothiazole as the acceptor and bithiophene and thieno[3,2-*b*]thiophene as the donors, respectively, are synthesized. These polymers have small band gaps (~1.2-1.3 eV) and low energy levels. When being used as channel semiconductors in organic thin film transistors, they show promising p-channel field effect transistor performance with hole mobility as high as 0.019 $cm^2V^{-1}s^{-1}$.

Introduction

Polymer semiconductors are important functional materials for printed electronics including organic thin film transistors (OTFTs) [1] and organic photovoltaics (OPVs).[2] Because of their certain advantages over traditional inorganic semiconductors such as solution processability, mechanical robustness, and light weight, they have great potential to be used in low cost and large area applications, including radio frequency identification tags (RFID), large area display, and solar cells. Donor-acceptor (D-A) semiconducting polymers, in which electron-donating and electron-accepting building blocks are alternatingly combined in the polymer backbone, are of extensive research interest recently.[1g,2-4] Great efforts have been made to explore new electron acceptors to obtain D-A copolymers with very high device performance. Thiazole is a heterocyclic structure frequently used in organic semiconductors and the introduction of thiazole moieties into organic semiconductors dates back to the 1990s.[5] Conjugated small molecules and polymers based on thiazole have been reported to exhibit high hole or electron mobilities in OTFTs. McCullough *et al*. reported air stable bithiazole[6] and thiazolothiazole[7] based copolymers that achieved hole mobilities of 0.14 and 0.3 $cm^2\ V^{-1}\ s^{-1}$, respectively. A small molecule semiconductor based on bithiazole was reported to show electron mobility as high as 1.83 $cm^2\ V^{-1}\ s^{-1}$ by Yamashita *et al*.[8] On the other hand, aromatic azo compounds with a -N=N- linkage are commonly used as commercial dyes. Some small azo molecules and polymers have been extensively investigated as promising materials for optical data storage and switching devices utilizing the photo-induced isomerization property of the azo moiety.[9-13] Recently, azobenzene derivatives were used as charge carrier traps in pentacene-based thin film transistors to induce electric bistability.[14] However, semiconducting polymers with azo moieties in the backbone were rarely synthesized[15-17]

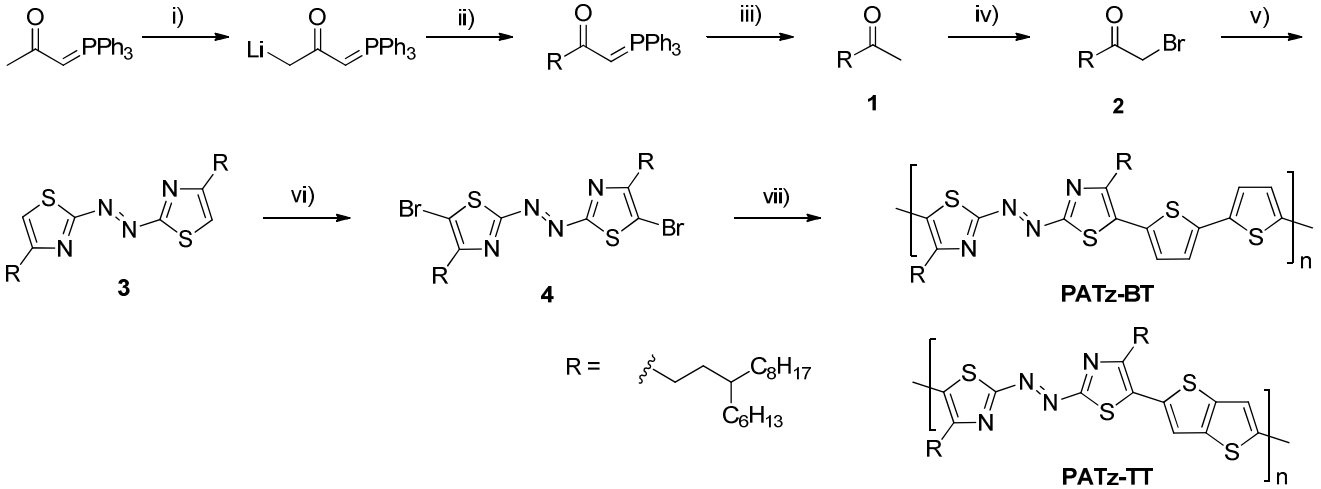

Scheme 1. Synthetic route to ATz-containing monomers and polymers: i) n-BuLi / THF / -78 °C; ii) 2-hexyldecylbromide/THF / 50 °C - r. t.; iii) H_2O/85 °C; iv) Br_2 / MeOH / -10 °C to r. t.; v) a) 2,5-dithiourea / EtOH / 50 °C, b) $NaNO_2$ / r. t; vi) Br_2 / $CHCl_3$ / 0 °C; vii) 5,5'-bis(trimethylstannyl)-2,2'-bithiophene (for **PATz-BT**) or 2,5-bis(trimethylstannyl)thieno[3,2-*b*]thiophene (for **PATz-TT**) / $Pd_2(dbda)_3$ / P(*o*-tolyl)$_3$ / chlorobenzene/90 °C.

and no azo-based polymer semiconductors have been reported as channel semiconductors for OTFTs. In this study, we synthesized a new azothiazole (ATz) (i.e., (*E*)-1,2-di(thiazol-2-yl)diazene) monomer for D-A polymers. Two common electron-donating building blocks, bithiophene and thieno[3,2-*b*]thiophene, were used to combine with the ATz building block to form DA polymers, **PATz-BT** and **PATz-TT** (Scheme 1). These polymers showed very narrow band gaps and exhibited characteristic p-channel field effect performance as channel semiconductors in OTFTs.

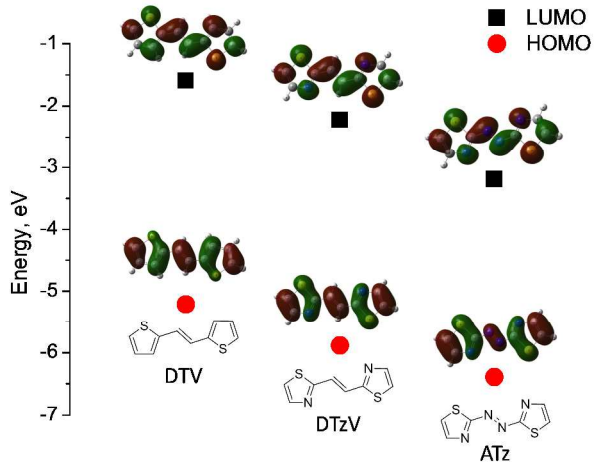

Figure 1. The HOMO and LUMO energy levels of azothiazole (ATz) and two of its structural analogues, (*E*)-1,2-di(thiophen-2-yl)ethene (DTV) and (*E*)-1,2-di(thiazol-2-yl)ethane (DTzV) calculated by computer simulations.

Results and Discussion

We started the study of the ATz-based D-A copolymers by conducting computer simulations on ATz and its two close structural analogues, (*E*)-1,2-di(thiophen-2-yl)ethene (DTV) and (*E*)-1,2-di(thiazol-2-yl)ethane (DTzV) (Figure 1). Geometry optimizations of these structures with minimum energy potential surfaces were performed with B3LYP/6-31G* basis set. All three molecules were found to be highly planar. The lowest unoccupied molecular orbital (LUMO) and the highest occupied molecular orbital (HOMO) energy levels of DTV were calculated to be -1.59 eV and -5.21 eV, respectively. With substitution of thiophene for thiazole, the resulting molecule DTzV possesses lower LUMO (-2.22 eV) and HOMO (-5.88 eV) levels due to the more electron accepting ability of thiazole than thiophene. When the central vinylene moiety of DTzV is further replaced with an azo unit, the obtained ATz structure showed significantly reduced LUMO and HOMO levels of -3.19 eV and -6.39 eV, respectively, indicating the strong electron accepting effect of the azo moiety. These simulation results suggest that ATz is a promising strong electron acceptor building block for donor-acceptor polymer semiconductors.

The synthesis of a dibrominated ATz monomer **4** and its copolymers, **PATz-BT** and **PATz-TT**, is depicted in Scheme 1. 5-Hexyltridecan-2-one (**1**) was synthesized from the reaction of 2-hexyldecylbromide with lithiotriphenylphosphinioacetonide. 1-Bromo-5-hexyltridecan-2-one (**2**) was then prepared via brominaition of 1. The azothiazole compound 1,2-bis(4-(3-hexylundecyl)thiazol-2-yl)diazene (**3**) was synthesized adopting a similar procedure used for the preparation of 4-methylazothiazole,[18-20] by reacting **2** with 2,5-dithiourea, followed by oxidation with sodium nitrite. **3** was then subjected to bromination with bromine to give 1,2-bis(5-bromo-4-hexylundecylthiazol-2-yl)diazene **4**. The long branched alkyl group is intended to render the resulting polymers soluble. **PATz-BT** and **PATz-TT** were synthesized via Stille-coupling polymerization of **4** with 5,5'-bis(trimethylstannyl)-2,2'-bithiophene and 2,5-bis(trimethylstannyl)thieno[3,2-*b*]thiophene, respectively. The crude polymers were purified with Sohxlet extraction using acetone, hexane, and dichloromethane to remove oligomers. The remaining polymers were dissolved with chloroform to afford **PATZ-BT** and **PATz-TT** in yields of 62% and 68%, respectively. Molecular weights of the polymers from the final chloroform fractions were measured using gel permeation chromatography (GPC) at a column temperature of 40 °C using THF as the eluent and polystyrene as the standards. Multiple elution peaks were observed for both polymers, indicating the presence of oligomers (see ESI). Other solvents such as ethyl acetate and toluene were used to remove lower molecular fractions using Sohxlet extraction, but no satisfactory results were obtained. The peak molecular weights (M_p) of the first elution peaks on the elution curves are 7.3kDa for **PATz-BT** and 46.1 kDa for **PATz-TT**.

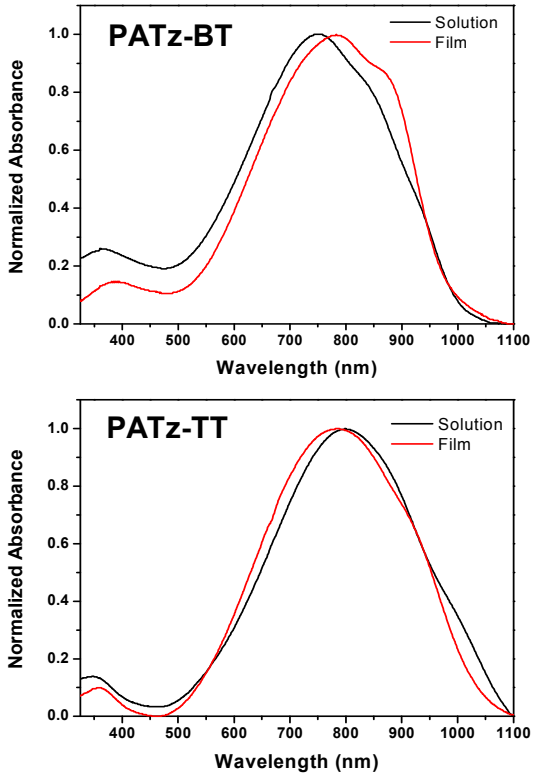

Figure 2. UV-vis-NIR spectra of **PATz-BT** and **PATz-TT** solutions (in chloroform) and as-spun films on glass substrates.

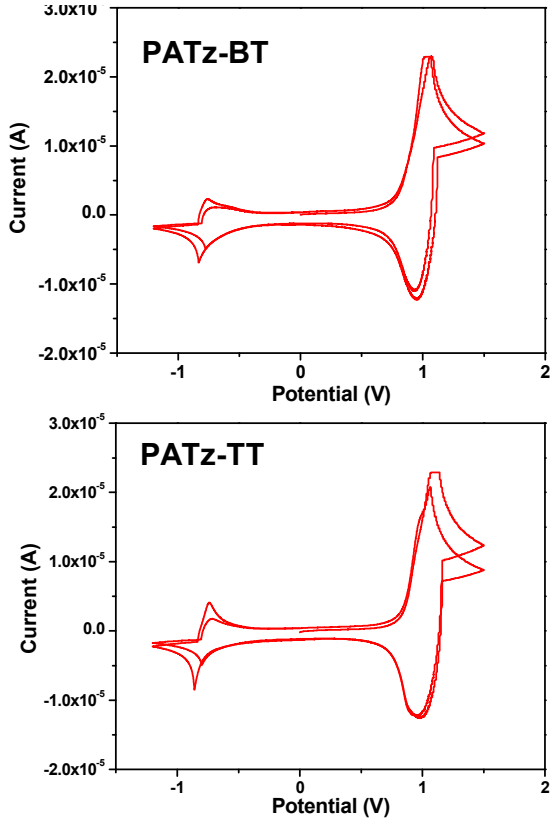

Figure 3. Cyclic voltammograms (two cycles) of **PATz-BT** and **PATz-TT** thin films showing two oxidative and reductive cycles obtained at a scan rate of 0.05 Vs^{-1} under argon. The electrolyte was 0.1 M tetrabutylammonium hexafluorophosphate in anhydrous acetonitrile.

Both polymers showed very broad absorption across the UV-Vis-NIR range (Figure 2). **PATz-BT** in chloroform exhibits a λ_{max} at 770 nm. In a solid thin film, **PATz-BT** showed a similar λ_{max} (~773 nm), but a shoulder at 862 nm was observed, which indicates a higher degree of chain ordering in the solid state. The spectrum for the film showed an onset wavelength of 979 nm, corresponding to an optical band gap of 1.27 eV. **PATz-TT** in chloroform exhibited a longer λ_{max} at 810 nm than that of **PATz-BT**. Interestingly, the **PATz-TT** film showed the λ_{max} at 770 nm, a 40 nm blue-shift from the solution spectrum. This blue shift phenomenon was also observed for other conjugated polymers,[21] which was explained by the formation of H-aggregates in the solid state.[21c-e] The optical band gap of **PDT-TT** was calculated to be ~1.22 eV from the absorption cut-off wavelength, which is lower than that of **PATz-BT**.

The redox properties of these ATz-based polymers were investigated by cyclic voltammetry (CV) to determine their HOMO and LUMO energy levels. The CV diagrams of two polymers showed reversible redox cycles, suggesting that they are stable towards both oxidation and reduction processes (Figure 3). Similar HOMO energy levels of ca. -5.5 eV were obtained for two polymers, while the LUMO levels were determined to be -4.1 eV for **PATz-BT** and -4.0 eV for **PATz-TT**, indicating that the

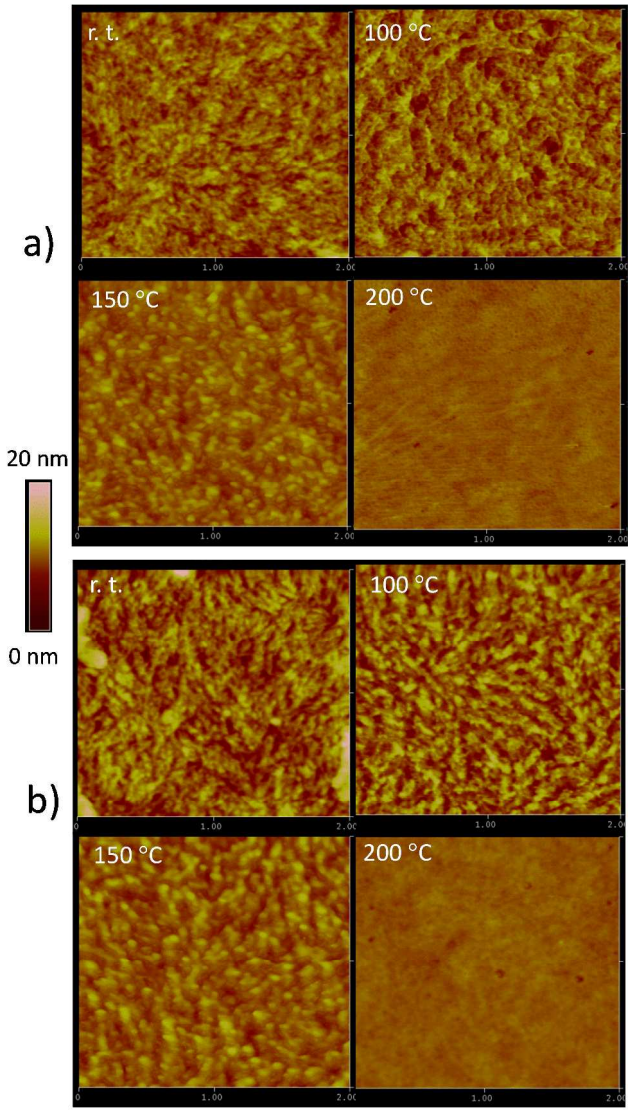

Figure 4. AFM height images (2 μm × 2 μm) of (a) PATz-BT and (b) PATz-TT thin films (~35 nm) spin-coated on dodecyltrichlorosilane (DTS)-modified SiO_2/Si substrates and optionally annealed at different temperatures for 15 min under nitrogen.

ATz building block is indeed a very strong electron acceptor.

The thermal stability of the polymers was examined by thermal gravimetric analysis (TGA). The 5% weight loss was observed at 304 °C and 287 °C for **PATz-BT** and **PATz-TT**, respectively (ESI). The rather low thermal stability of these polymers is considered due to the thermally labile azo moiety, which would undergo thermal decomposition to liberate nitrogen gas.[22] The thermal decomposition behavior of these polymers was further verified by differential scanning calorimetry (DSC) measurements (ESI). The DSC curves of **PATz-BT** and **PATz-TT** showed exothermic peaks at 240 and 243 °C, respectively, during the first heating scans, which are most likely due to the decomposition of the polymers. There were no any thermal transitions observed in the subsequent cooling scan and the second heating-cooling cycles, which further confirmed the decomposition of the polymers.

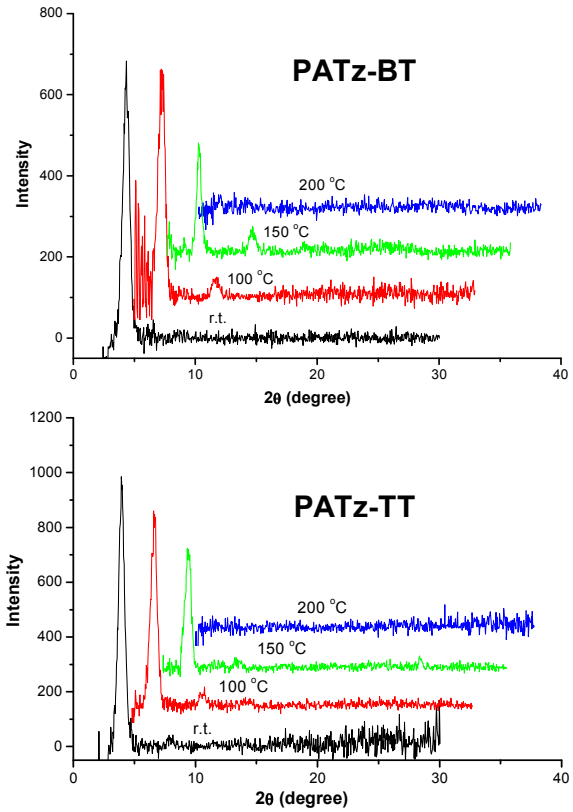

Figure 5. X-ray diffraction (XRD) data obtained from spin-coated polymer thin films on DTS-modified SiO_2/Si substrates optionally annealed at different temperatures.

The surface morphology of the polymer thin films was investigated using atomic force microscopy (AFM). The morphological features of the **PATz-BT** and **PATz-TT** films change with increasing annealing temperature (Figure 4). Distinct grains were observed for both polymers at an annealing temperature of 150 °C. At an annealing temperature of 200 °C, both polymers showed smooth featureless morphology, which is most likely caused by the thermal decomposition of these polymers.

The molecular ordering in polymer thin films was characterized using XRD. For the as-spun **PATz-BT** thin film, a peak at 2θ = 4.35°, corresponding to a d-spacing of 2.03 nm was observed (Figure 5). This peak represents the interlayer distance of a lamellar crystal structure, which has been frequently reported for other crystalline conjugated polymers.[3,4] Since there is no diffraction peak reflecting the co-facial π-π distance, this polymer presumably adopted an edge-on chain orientation. After annealing at 100 °C, the secondary diffraction peak at 2θ = 8.74° appeared, which suggests that a longer range of chain ordering formed upon annealing. Increasing the annealing temperature to 150 °C led to a slight decrease in the interlayer distance to 1.94 nm (2θ = 4.55°). The diffraction intensity of the primary peak also weakened, which is likely due to the partial thermal decomposition of the polymer. Further increasing annealing temperature to 200 °C caused serious degradation of the polymer and no diffraction peaks were observed. The as-spun **PATz-TT** film showed a slightly larger interlayer spacing (2θ = 3.92°, d = 0.225 nm) than that of **PATz-BT**. In the diagram of the 100 °C-annealed **PATz-TT** film, the second order diffraction peak at 2θ = 7.83° appeared, indicating its longer range of ordering due to annealing. Similar to **PATz-BT**, the **PATz-TT** films showed no diffraction peaks as the annealing temperature increased to 200 °C due to decomposition of this polymer.

PATz-BT and **PATz-TT** were evaluated as channel semiconductors in bottom-contact bottom-gate OTFTs on heavily n-doped Si wafer with a thermally grown SiO_2 dielectric layer (~300 nm). Thermally evaporated gold was used as the drain and source electrodes and the doped silicon wafer support functioned as the gate electrode. Polymer thin films were deposited by spin coating a polymer solution in chloroform onto the dodecyltrichlorosilane (DTS)-modified SiO_2 dielectric layer in a glove box filled with nitrogen. Since these polymers decompose beyond 200 °C, the maximum annealing temperature was 150 °C. The devices were measured in a glove box after cooling.

OTFT devices with the non-annealed **PATz-BT** thin films showed typical p-channel field effect performance (Figure 6) with good hole mobility in the range of 1.0-1.3 × 10^{-2} $cm^2V^{-1}s^{-1}$ along a current on-to-off ratio (I_{on}/I_{off}) of ~10^3-10^4 (Table 1). Upon annealing at 100 °C, the **PATz-BT** thin films showed improved mobility up to 1.4-1.9×10^{-2} $cm^2V^{-1}s^{-1}$ due to the higher degree of chain ordering in the annealed films as supported by the XRD data. Further increasing the annealing temperature to 150 °C led no obvious change in mobility (1.5-1.8×10^{-2} $cm^2V^{-1}s^{-1}$). All OTFTs fabricated with **PATz-TT** also exhibited hole transport characteristics. However, the mobility values obtained for **PATz-TT** are slightly lower than those of **PATz-BT**. The best mobility of value achieved for **PATz-TT** is 1.5×10^{-2} $cm^2V^{-1}s^{-1}$ for a device with a 100 °C-annealed polymer film. The slightly poorer performance observed for **PATz-TT** is considered to be due to

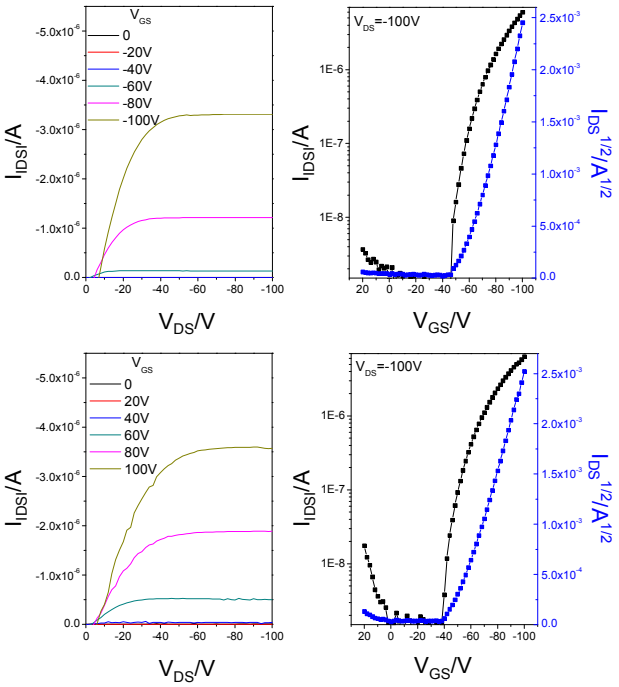

Figure 6. Output and transfer curves of typical OTFT devices with PATz-BT film (top) and PATz-TT film (bottom) annealed at 100 °C. Device dimensions: channel length (L) = 30 μm; channel width (W) = 1 mm.

the presence of a significant amount of oligomers. Considering very low molecular weight of **PATz-BT** (M_n = 7.3 kDa) and the presence of a large amount of oligomers in **PATz-TT**, the field effect performance of these ATz polymers is expected to improve notably if the molecular weight can be further increased[3b,3g] upon optimization of polymerization conditions. All OTFT devices using **PATz-BT** and **PATZ-TT** showed quite high threshold voltage values, which indicates the presence of a large number of trapping sites in the semiconductor layer[23] or at the semiconductor/dielectric interface.[24]

Table 1 Summary of device performance parameters of OTFT devices based on **PATz-BT** and **PATz-TT**.

Polymer	Annealing temperature (°C)	μ_h ($cm^2V^{-1}s^{-1}$)[a]	V_T(V)[b]	I_{on}/I_{off}[c]
PATz-BT	None	$1.0 – 1.3\times10^{-2}$	-43 – -57	$\sim10^3–10^4$
	100	$1.4 – 1.9\times10^{-2}$	-60 – -63	$\sim10^3–10^4$
	150	$1.5 – 1.8\times10^{-2}$	-58 – -62	$\sim10^3–10^4$
PATz-TT	None	$3.5 – 5.7\times10^{-3}$	-39 – -53	$\sim10^3–10^4$
	100	$1.0 – 1.5\times10^{-2}$	-46 – -57	$\sim10^3–10^4$
	150	$4.1 – 6.4\times10^{-3}$	-47 – -54	$\sim10^3–10^4$

[a] Mobility calculated from the saturation region at a drain-source voltage (V_{DS}) of -100 V. [b] The threshold voltage. [c] The current on/off ratio.

Experimental

Materials and Characterization

All chemicals were purchased from Sigma-Aldrich and other commercial sources and used without further purification. Geometry optimizations of azothiazole (ATz) (i.e., (*E*)-1,2-di(thiazol-2-yl)diazene), (*E*)-1,2-di(thiophen-2-yl)ethene (DTV), and (*E*)-1,2-di(thiazol-2-yl)ethane (DTzV) were performed with density functional theory (DFT) calculation using the B3LYP hybrid functional[25,26] with the 6-31G* basis set. Molecular orbital shapes and energies discussed in the text are those calculated at the optimized structures. Orbital pictures were prepared with GaussView 5.0 software.[27] All calculations were performed with Gaussian 09 package[28] on the Shared Hierarchical Academic Research Computer Network (SHARCNET) of Canada. NMR data were collected on a Bruker DPX 300 MHz spectrometer with chemical shifts relative to tetramethylsilane (TMS, 0 ppm). UV-Vis spectra were recorded on a Thermo Scientific model GENESYS^{TM} 10S VIS Spectrophotometer. Thermal gravimetric analysis (TGA) was carried out using a TGA Q500 (TA Instruments) at a heating rate of 10 °C min^{-1} under nitrogen. Cyclic voltammograms (CV) were obtained with a Digi-Ivy model DY2111 Potentiostat using an Ag/AgCl reference electrode, a platinum foil counter electrode and a platinum disk working electrode. The polymer film was coated on the working electrode by drop-casting a polymer solution. CV measurements were collected in 0.1 M tetrabutylammonium hexafluorophosphate in dry acetonitrile using the ferrocene/ferrocenium (Fc/Fc+) couple as a standard at a scan rate of 50 mV s^{-1} under argon. The HOMO and LUMO energy levels were calculated using the equation $E_{HOMO} = -(E_{ox} - E_{Fc/Fc^+}) - 4.8$ eV and $E_{LUMO} = -(E_{red} - E_{Fc/Fc^+}) - 4.8$ eV, where E_{ox} and E_{red} are the onset oxidation and reduction potentials of the polymer sample against the Ag/AgCl reference electrode, E_{Fc/Fc^+} is the onset oxidation potential of ferrocene against the Ag/AgCl reference electrode, and -4.80 eV is the HOMO energy level of ferrocene with respect to the vacuum level (0 eV).[29] XRD measurement are carried out with a Bruker D8 Advance powder diffractometer with Cu Kα1 radiation (λ = 1.5406 Å) using standard Bragg-Brentano geometry. AFM images were obtained on polymer thin films spin coated on dodecyltrichlorosilane (DTS)-modified SiO_2/Si substrates using a Dimension 3100 Scanning Probe Microscope. Gel permeation chromatography (GPC) measurement of polymers was performed on a Waters 2690 system using THF as the eluent and polystyrene as standards at a column temperature of 40 °C. Elemental analysis (EA) was performed on an Elementar Vario EL Cube elemental analyser. High resolution electron ionization (HREI) MS spectra were obtained on a Waters/Micromass GCT Time-of-flight mass spectrometer. The positive ion mode high resolution electron spray ionization (HRESI) MS spectra were obtained on a Waters/Micromass QToF Global Ultima Time-of-flight mass spectrometer.

Fabrication and Characterization of OTFT devices.

A bottom-contact bottom-gate OTFT configuration was used. Heavily n-doped Si wafer was used for fabricating OTFTs. Si wafer functions as the gate electrode and a thermally grown SiO_2 dielectric. Au source and drain electrode pairs were pre-deposited on the SiO_2 layer using a conventional photolithography method. The substrate was cleaned with de-ionized (DI) water, acetone, and isopropanol in an ultrasonic bath, followed by air plasma treatment. Subsequently, the substrate was immersed in a DTS solution in toluene (10 mg/mL) at 70 °C for 20 min. After washing with toluene, the substrate was dried under a nitrogen flow. A polymer solution in chloroform (10 mg mL^{-1}) was spin coated on the substrate at 3000 rpm for 60 s to give a polymer film, which was optionally subjected to thermal annealing at different temperatures for 15 min in a glove box. OTFT devices have a channel length (L) of 30 μm and a channel width (W) of 1000 μm. The devices were characterized in a glove box using an Agilent B2912A Semiconductor Analyser. The carrier mobility in the saturated regime, μ_{sat}, was calculated using the equation of $I_{DS} = C_i\mu_{sat}(W/2L)(V_G - V_T)^2$, where I_{DS} is the drain current, C_i is the capacitance per unit area of the gate dielectric, W and L are, respectively, the semiconductor channel width and length, and V_{GS} and V_T are, respectively, the gate voltage and threshold voltage. V_T of the devices was determined by extrapolating the linear fit of the $(I_{DS})^{1/2}$ versus V_{GS} curve in the saturation regime at $I_{DS} = 0$.

Synthetic procedures

Synthesis of 5-hexyltridecan-2-one (1): n-BuLi (2.5 M in hexane, 2.5 mL, 6.26 mmol) was added dropwise into a suspension of 1-(triphenylphosphoranylidene)propan-2-one (2.05 g, 6.44 mmol) in anhydrous THF (50 mL) at -78 °C under argon. The reaction mixture was stirred for 15 min at -78 °C. 2-Hexyldecylbromide (1.82 g, 5.96 mmol) was added dropwise. After addition, the cold bath was replaced by an ice-water bath and the reaction mixture was kept at 0 °C for 4 h and then

allowed to warm up to room temperature and stirred overnight. Solvent was evaporated and 30 mL of ethanol was added into the residue. Water was added to approach the cloud point. The mixture was then heated at 85 °C overnight. After cooling down to room temperature, the mixture was poured into DI water (50 mL) and extracted with hexane (2 × 50 mL). The combined organic phase was dried over anhydrous $MgSO_4$, filtered, and subject to a reduced pressure to remove the solvent. The residue was passed through a silica gel pad using hexane to remove the unreacted 7-(bromomethyl)pentadecane). The silica gel pad was then washed with chloroform, and the chloroform eluent was concentrated under a reduced pressure to yield 5-hexyltridecan-2-one as a yellow liquid (0.6056 g, 36 %). ^{1}H NMR (300 MHz, $CDCl_3$): δ 2.44-2.33 (t, J = 7.5 Hz, 2H), 2.14 (s, 3H), 1.57-1.47 (m, 2H), 1.26 (s, 25H), 0.88 (t, J = 6.5 Hz, 6H). HREI (M) Calc. for $C_{19}H_{38}O$: 282.2915; found: 282.2923. Elemental analysis: Calc. for $C_{19}H_{38}O$: C 80.78, H 13.56%; found: C 81.23, H 13.65%.

Synthesis of 1-bromotridecan-2-one (2): Bromine (4.08 g, 25.56 mmol) was added dropwise to a solution of **1** (7.22 g, 25.56 mmol) in methanol (40 mL) at -20 °C with stirring. The mixture was allowed to warm to room temperature over a period of 2 h. After stirring at room temperature for an additional hour, the mixture was cooled down to 0 °C. Water (6 mL) and concentrated sulphuric acid (14 mL, 98% wt) were added and the mixture was allowed to warm to room temperature and stirred overnight. The mixture was poured into water (75 mL) and extracted with hexane three times. The combined organic phase was dried over anhydrous $MgSO_4$ and filtered. After removing solvent, the residue was purified through column chromatography on silica gel with hexane: dichloromethane (2:1) to afford the product. Yield: 3.23 g (35 %). ^{1}H NMR (300 MHz, $CDCl_3$): δ 3 3.87 (s, 2H), 2.60 (t, J = 7.8 Hz, 2H), 1.61 – 1.53 (m, 2H), 1.24 (s, 15H), 0.86 (t, J = 6.3 Hz, 6H). ^{13}C NMR (75 MHz, $CDCl_3$): δ 202.61, 37.32, 36.96, 34.26, 33.36, 31.92, 31.89, 30.05, 29.71, 29.63, 29.34, 27.61, 26.57, 26.54, 22.69, 14.11. HREI (M-Br)$^+$ Calc. for $C_{19}H_{37}O^+$: 281.2833; found: 281.2844. Elemental analysis: Calc. for $C_{19}H_{37}BrO$: C 63.14, H 10.32%; found: C 62.58, H 9.72%.

Synthesis of 1,2-bis(4-(3-hexylundecyl)thiazol-2-yl)diazene (3): Compound **2** (1.38 g, 3.82mmol) and 2,5-dithiobiurea (0.287 g, 1.91 mmol) were heated in ethanol (6 mL) at 50 °C for 2.5 h under argon. The mixture was then cooled to room temperature and stirred overnight. Ethyl acetate was then added into the mixture to obtain a white solid, which was collected by filtration, washed with small amounts of ethanol and ethyl acetate, and briefly dried. The resulting solid was then stirred in 20 mL of ethyl acetate and 40 mL of water. An aqueous solution of $NaNO_2$ (0.13 g, 1.91 mmol) was added dropwise into the reaction mixture and the mixture was stirred for 1 h. After phase separation using ethyl acetate and water, the combined organic phase was dried over anhydrous $MgSO_4$, filtered, and subjected to evaporation of solvent under reduced pressure. The residue was purified through column chromatography on silica gel (hexane:dichloromethane, 2:1) to give an orange solid (0.73g, 75 %). ^{1}H NMR (300 MHz, $CDCl_3$): δ 7.14 (s, 2H), 2.86 (t, J = 8.1Hz, 4H), 1.83-1.66 (m, 4H), 1.56-1.00 (m, 50H), 0.88 (t, J = 6.4 Hz, 12H). ^{13}C NMR (75 MHz, $CDCl_3$): δ 174.08, 160.67, 117.88, 37.10, 33.38, 33.04, 31.80, 30.00, 29.66, 29.54, 29.25, 26.51, 26.48, 22.58, 22.57, 14.00. HRESI (M+H)$^+$ Calc. for $C_{40}H_{73}N_4S_2^+$: 673.5291; found: 673.5277. Elemental analysis: Calc. for $C_{40}H_{72}N_4S_2$: C 71.37, H 10.78, N 8.32%; found: C 71.67, H 10.72, N 8.18%.

Synthesis of 1,2-bis(5-bromo-4-hexylundecylthiazol-2-yl)diazene (4): Compound **4** was synthesized similarly according to the procedure described for the preparation of 1,2-bis(5-bromo-4-methylthiazol-2-yl)diazene.[30] Compound **3** (1.0662 g, 1.58 mmol) was dissolved in 80 mL of chloroform and cooled in an ice-water bath. A bromine (0.506 g, 3.17 mmol) solution in chloroform (5 mL) was added dropwise at 0 °C in the dark. The mixture was stirred for 5 h at 0 °C after addition of the bromine solution, and poured into water (40 mL). After extraction with dichloromethane, the combined organic phase was washed with dilute $Na_2S_2O_3$ solution, dried over anhydrous Na_2SO_4, filtered and subject to evaporation of solvent under a reduced pressure. The residue was purified through column chromatography on silica gel (hexane : toluene, 3 : 1) to afford **4**. Yield: 0.3618 g (28 %). ^{1}H NMR (300 MHz, $CDCl_3$): δ 2.83(t, J = 8.1 Hz, 4H), 1.73 (m, 4H), 1.17-1.43 (m, 32H), 0.88 (t, J = 6.1 Hz, 12H). ^{13}C NMR (75 MHz, $CDCl_3$): δ 172.52, 159.66, 113.20, 37.27, 33.43, 32.43, 31.94, 30.12, 29.78, 29.69, 29.39, 27.39, 26.59, 22.72, 14.15. HRESI (M+H)$^+$ Calc. for $C_{40}H_{71}Br_2N_4S_2^+$: 829.3495; found: 829.3487. Elemental analysis: Calc. for $C_{40}H_{70}Br_2N_4S_2$: C 57.82, H 8.49, N 6.74%; found: C 58.19, H 8.49, N 6.65%.

Synthesis of PATz-BT: A 100 mL dry two-neck round bottom flask was charged with **4** (0.289 g, 0.348 mmol), 5,5'-bis(trimethylstannyl)-2,2'-bithiophene (0.171 g, 0.348 mmol), and tri(*o*-tolyl)phosphine (8.5 mg, 0.028 mmol). The vessel was evacuated and filled with argon three times. After addition of anhydrous chlorobenzene (10 mL) and tris(dibenzylideneacetone)dipalladium (6.4 mg, 0.007 mmol), the mixture was heated at 90 °C under argon for 72 h. Then bromobenzene (0.5 mL) was added, and the reaction mixture was heated for another 12 h at 90 °C. After cooling down to room temperature, the reaction mixture was added into acetone (150 mL) under stirring. The polymer was collected by filtration and purified through Soxhlet extraction using methanol, acetone, hexane, dichloromethane, and chloroform. Yield: 0.182 g (62.0 %) from the chloroform fraction.

Synthesis of PATz-TT: PATz-TT was prepared via Stille coupling of **4** with 2,5-bis(trimethylstannyl)thieno[3,2-*b*]thiophene according the procedure described above for the preparation of **PATz-BT**. The polymer was purified by Soxhlet extraction using methanol, acetone, hexane, dichloromethane, and chloroform. Yield: 0.187 g (68 %) from the chloroform fraction.

Conclusions

In this study, we reported the first use of azothiazole as an electron accepting building block to construct polymer semiconductors. Two copolymers based on azothiazole, **PATz-BT** and **PATz-TT**, were prepared. These polymers have low-

lying LUMO energy levels at ca.-4 eV, indicating the very strong electron withdrawing effect of the azothiazole moiety. **PATz-BT** and **PATz-TT** exhibited hole transport performance with hole mobility as high as ~1.9 × 10^{-2} $cm^2V^{-1}s^{-1}$ despite their low molecular weight and the presence of a large amount of oligomers. These azothiazole based polymer semiconductors showed small bandgaps of ~1.2-1.3 eV with very broad absorption profiles covering the UV-Vis-IR range, making these polymers potentially useful as donor materials for organic photovoltaics.

Acknowledgments

The authors thank Natural Sciences and Engineering Research Council (NSERC) of Canada for financial support (Discovery Grants) of this research, and Toufic N. Aridi and Prof. Mario Gauthier of University of Waterloo for the GPC measurements. The authors also thank Angstrom Engineering Inc. for providing the thermal deposition system for the fabrication of OTFT devices.

Notes and references

[a] *Department of Chemical Engineering and Waterloo Institute for nanotechnology (WIN), University of Waterloo, 200 University Ave West ON, Waterloo, Canada, N2L 3G1. Fax: 1-519-888-4347; Tel: 1-519-888-4567 ext. 31105; E-mail: yuning.li@uwaterloo.ca*

† Electronic Supplementary Information (ESI) available: NMR, GPC, TGA, DSC, and additional OTFT data. . See DOI: 10.1039/b000000x/

1 (a) C. R. Kagan, D. B. Mitzi and C. D. Dimitrakopoulos, *Science,* 1999, **286**, 945. (b) C. D. Dimitrakopoulos and P. R. L. Malenfant , *Adv. Mater.,* 2002, **14**, 99; (c) S. R. Forrest, *Nature*, 2004, **428**, 911. (d) H. Sirringhaus, *Adv. Mater.,* 2005, **17**, 2411. (e) B. S. Ong, Y. Wu, Y. Li , P. Liu, H. Pan, *Eur. J. Chem.,* 2008, **14**, 4766 (f) C. Wang, H. Dong, W. Hu, Y. Liu and D. Zhu, *Chem. Rev.*, 2012, **112**, 2208. (g) C. Guo, W. Hong, H. Aziz and Y. Li, *Rev. Adv. Sci. Eng.*, 2012, **1**, 200. (h) X. Zhao and X. Zhan, *Chem. Soc. Rev.*, 2011, **40**, 3728. (i) A. Facchetti, *Chem. Mater.*, 2011, **23**, 733. (j) A. C. Arias, J. D. MacKenzie, I. McCulloch, J. Rivnay and A. Salleo, *Chem. Rev.,* 2010, **110**, 3. (k) Y. Li, P. Sonar, L. Murphy and W. Hong, *Energy Environ.Sci.,* 2013, **6**, 1684. (l) C. B. Nielsen, M. Turbiez and I. McCulloch*, Adv. Mater.*, 2013, **25**, 1859.

2 (a) Chen, J.; Cao, Y. *Acc. Chem. Res*. **2009**, *42*, 1709. (b) Cheng, Y. J.; Yang, S. H.; Hsu, C. S. *Chem. Rev.* **2009**, *109,* 5868. (c) Boudreault, P. T.; Najari, A.; Leclerc, M. *Chem. Mater.* **2011**, *23*, 456. (d) Kularatne, R. S.; Magurudeniya, H. D.; Sista, P.; Biewer, M. C.; Stefan, M. C. *J. Polym. Sci., Part A: Polym. Chem.* **2013**, *51*, 743.

3. (a) Y. Li, S. P. Singh and P. Sonor, *Adv. Mater*., 2010, **22**, 4862. (b) Y. Li, P. Sonar, S. P. Singh, M. S. Soh, M. Meurs and J. Tan, *J. Am. Chem. Soc*., 2011, **133**, 2198. (c) Y. Li, P. Sonar, S. P. Singh, Z. Zeng, M. S. Soh, *J. Mater. Chem*., 2011, **21**, 10829. (d) P. Sonar, S. P. Singh, Y. Li, Z. Ooi, T. Ha, I. Wong, M. S. Soh and A. Dodabalapur, *Energy Environ. Sci*., 2011, **4**, 2288. (e) H. Chen, Y. Guo, G. Yu, Y. Zhao, J. Zhang, D. Gao, H. Liu and Y. Liu, *Adv. Mater.*, 2012, **24**, 4618. (f) B. Sun, W. Hong, H. Aziz, N. M. Abukhdeir and Y. Li, *J. Mater. Chem. C*, 2013, **1**, 4423.(g) J. Li, Y. Zhao, H. S. Tan, Y. Guo, C.-A. Di, G. Yu, Y. Liu, M. Lin, S. H. Lim, Y. Zhou, H. Su and B. S. Ong, *Sci. Rep*., 2012, **2**, 754.

4. (a) T. Lei, Y. Cao, Y. Fan, C.-J. Liu, S.-C. Yuan and J. Pei, *J. Am. Chem. Soc.*, 2011, **133**, 6099. (b) J. Mei, D. H. Kim, A. L. Ayzner, M. F. Toney and Z. Bao, *J. Am. Chem. Soc.,* 2011, **133**, 20130. (c) T. Lei, J.-H. Dou, Z.-J. Ma, C.-H. Yao, C.-J. Liu, J.-Y. Wang and J. Pei, *J. Am. Chem. Soc*., 2012, **134**, 20025.

5. Y. Lin, H. Fan, Y. Li, and X. Zhan, *Adv. Mater.*, 2012, **24**, 3087.

6. J. Liu, R. Zhang, I. Osaka, S. Mishra, A. E. Javier, D.-M. Smilgies, T. Kowalewski, and R. D. McCullough, *Adv. Funct. Mater.*, 2009, **19**, 3427.

7. I. Osaka, G. Sauvé, R. Zhang, T. Kowalewski, and R. D. McCullough, *Adv. Mater.*, 2007, **19**, 4160.

8. S. Ando, R. Murakami, J. Nishida, H. Tada, Y. Inoue, S. Tokito, and Y. Yamashita, *J. Am. Chem. Soc.*, 2005, **127**, 14996.

9. G. G. Nair, S. K. Prasad, and C. V. Yelamaggad, *J. Appl. Phys.*, 2000, **87**, 2084.

10. A. Natansohn and P. Rochon, *Chem. Rev.*, 2002, **102**, 4139.

11. T. Ikeda, J. Mamiya, and Y. Yu, *Angew. Chem. Int. Ed.*, 2007, **46**, 506.

12. S. Xie, A. Natansohn, and P. Rochon, *Chem. Mater.*, 1993, **5**, 403.

13. Y. Yu, M. Nakano, and T. Ikeda, *Nature*, 2003, **425**, 145.

14. C.-W. Tseng, D.-C. Huang, and Y.-T. Tao, *ACS Appl. Mater. Interfaces*, 2012, **4**, 5483.

15. P. Imin, M. Imit, and A. Adronov, *Macromolecules*, 2012, **45**, 5045.

16. A. Izumi, M. Teraguchi, R. Nomura, and T. Masuda, *J. Polymer Sci. A*, 2000, **38**, 1057.

17. W. Zhang, K. Yoshida, M. Fujiki, and X. Zhu, *Macromolecules*, 2011, **44**, 5105.

18. D. Markees, M. Kellerhals, and H. Erlenmeyer, *Helv. Chim. Acta*, 1947, **30**, 304.

19. H. Beyer, H. Schulte, and G. Henseke, *Chem. Ber.*, 1949, **82**, 143.

20. H. Beyer and A. Kreutzberger, *Chem. Ber.*, 1952, **85**, 333.

21 (a) J. Mei, D. H. Kim, A. L. Ayzner, M. F. Toney and Z. Bao, *J. Am. Chem. Soc.*, 2011, **133**, 20130. (b) R. S. Ashraf, A. J. Kronemeijer, D. I. James, H. Sirringhaus and I. McCulloch, *Chem. Commun*., 2012, **48**, 3939. (c) C. Scharsich, R. H. Lohwasser, M. Sommer, U. Asawapirom, U. Scherf, M. Thelakkat, D. Neher and A. Köhler, *J. Polym. Sic., Part B: Polym. Phys*. 2012, **50**, 442. (d) J. Lee, A.-R. Han, J. Kim, Y. Kim, J. H. Oh and C. Yang, *J. Am. Chem. Soc*., 2012, **134**, 20713. (e) J. Shin, H. A. Um, D. H. Lee, T. W. Lee, M. J. Cho and D. H. Choi, *Polym. Chem*., 2013, **4**, 5688.

22. (a) J. P. Van Hook and A. V. Tobolsky, *J. Am. Chem. Soc.*, 1958, **80**, 779–782. (b) C.-H. S. Wu, G. S. Hammond, and J. M. Wright, *J. Am. Chem. Soc.*, 1960, **82**, 5386. (c) F. M. Lewis and M. S. Matheson, *J. Ame. Chem. Soc.*, 1949, **71**, 747.

23. T. Hallam, M. Lee, N. Zhao, I. Nandhakumar, M. Kemerink, M. Heeney, I. McCulloch and H. Sirringhaus, *Phys. Rev. Lett*., 2009, **103**, 256803.

24. S. D. Wang, T. Miyadera, T. Minari, Y. Aoyagi and K. Tsukagoshi, *Appl. Pjys. Lett.*, 2008, **93**, 043311.

25. A. Becke, *Phys. Rev. A*, 1988, **38**, 3098.

26. C. Lee, W. Yang, and R. G. Parr, *Phys. Rev. B*, 1988, **37**, 785.

27. Æ. Frisch, H. P. Hratchian, R. D. Dennington II, T. A. Keith, J. Millam, A. B. Nielsen, A. J. Holder, and J. Hiscocks, *GaussView 5 Reference*, Wallingford, CT, Manual Ver., 2009.

28. Æ. Frisch, *Gaussian 09W Reference*, Wallingford, CT, 2009.

29. (a) M. Kumada and K. Tamao, *Adv. Organomet. Chem.*, 1968, **6**, 19. (b) J. Pommerehne, H. Vestweber, W. Guss, R. F. Mahrt, H. Bassler, M. Porsch and J. Daub, *Adv. Mater.,* 1995, **7**, 551. (c) M. Al-Ibrahim, H. K. Roth, M. Schroedner, A. Konkin, U. Zhokhavets, G. Gobsch, P. Scharff and S. Sensfuss, *Org. Electron.,* 2005, **6**, 65.

30. P. Holt and A. Smith, *J. Chem. Soc.*, 1965, 5245.